Inorganic Chemistry

Article

pubs.acs.org/IC

The $[U_2(\mu\text{-}S_2)_2Cl_8]^{4-}$ Anion: Synthesis and Characterization of the Uranium Double Salt $Cs_5[U_2(\mu\text{-}S_2)_2Cl_8]I$

Matthew D. Ward,[†] Eric A. Pozzi,[†] Minseong Lee,[‡] Richard P. Van Duyne,[†] Eun Sang Choi,[‡] and James A. Ibers*[,†]

[†]Department of Chemistry, Northwestern University, Evanston, Illinois 60208-3113, United States

[‡]Department of Physics and National High Magnetic Field Laboratory, Florida State University, Tallahassee, Florida 32310-3706, United States

Supporting Information

ABSTRACT: Red plates of $Cs_5[U_2(\mu\text{-}S_2)_2Cl_8]I$ were obtained in good yield from the reaction at 1173 K of U, GeI_2 or SnI_4, and S, with CsCl flux. The compound crystallizes in space group D_{2h}^{25}-*Immm* of the orthorhombic system in the $Cs_5[Nb_2(\mu\text{-}S_2)_2Cl_8]Cl$ structure type. The centrosymmetric $[U_2(\mu\text{-}S_2)_2Cl_8]^{4-}$ anion in the structure has *mmm* symmetry with the two U^{4+} atoms separated by 3.747(1) Å. Each U atom is coordinated to four Cl atoms and four S atoms from two S_2^{2-} groups in a square-antiprismatic arrangement. The polarized absorbance spectra of $Cs_5[U_2(\mu\text{-}S_2)_2Cl_8]I$ display prominent optical anisotropy. Magnetic measurements are consistent with the modified Curie–Weiss law at high temperatures. The low-temperature behavior may arise from antiferromagnetic coupling of the U^{4+} ions within the anion.

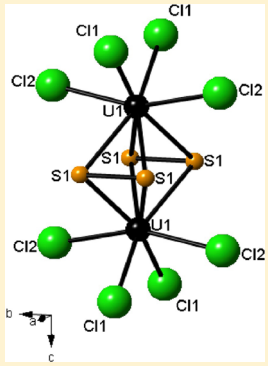

INTRODUCTION

Ternary and quaternary actinide chalcogenides have been the subject of continued research, and a large library of compounds is now known, especially for U.[1−4] This library includes a number of compounds that show interesting physical properties.[5−8] Expanding this library to include quaternary and especially quintary compounds is difficult owing to the stability of phases containing fewer elements. Examples of quintary U compounds include $CsLiU(PS_4)_2$,[9] $Ba_7UM_2S_{12.5}O_{0.5}$,[10] $UTa_2O(S_2)_3Cl_6$,[11] and $Na_2Ba_2(UO_2)S_4$.[12] The latter contains the unusual U^{6+} anion $[(UO_2)S_4]^{6-}$.

Actinide chalcohalides, An/Q/X (An = actinide; Q = chalcogen; X = halide), are virtually unexplored in comparison with An/Q compounds, with only six compounds being reported. These compounds are $[Hg_3Te_2][UCl_6]$,[13] $[Ta_7(Se_2)_{14}][U_2I_{10}]_2$,[14] $Te_8[U_2Br_{10}]$,[15] $UTa_2O(S_2)_3Cl_6$,[11] $[SCl_3][UCl_6]$,[16] and $ThTe_2I_2$.[17] Synthesis of An/Q/X compounds is complicated by the stability of both binary An/Q and A/X phases.

Here we report the synthesis and characterization of a new An/Q/X quintary, $Cs_5[U_2(\mu\text{-}S_2)_2Cl_8]I$, a double salt of U^{4+} containing the new $[U_2(\mu\text{-}S_2)_2Cl_8]^{4-}$ anion.

EXPERIMENTAL METHODS

Synthesis. Red plates of $Cs_5[U_2(\mu\text{-}S_2)_2Cl_8]I$ were obtained from the reaction of U (0.0300 g, 0.126 mmol), GeI_2 (0.0411 g, 0.131 mmol), S (0.0121 g, 0.377 mmol), and CsCl flux (0.0750 g, 0.445 mmol). The reactants were loaded into a carbon-coated fused-silica tube under an inert Ar atmosphere and then evacuated to 10^{-4} Torr. The tube was flame-sealed. It was then loaded into a computer-controlled furnace and heated to 1173 K in 12 h, held there for 6 h, cooled to 1073 K over 12 h, and held at 1073 K for 96 h. The reaction was cooled to 773 at 5 K/h and then cooled to 298 K in a further 12 h. The reaction afforded red plates of $Cs_5[U_2(\mu\text{-}S_2)_2Cl_8]I$ in about 75 wt % yield (based on Cl) as well as excess flux and Ge/S binaries. A few crystals were manually extracted from the resulting product and stored under Paratone oil. Elemental analysis of the crystals using a Hitachi 3400 SEM equipped for EDX analysis revealed the presence of Cs:U:S:Cl:I in an approximate ratio of 5:2:4:8:1. Importantly, no Ge was detected. $Cs_5[U_2(\mu\text{-}S_2)_2Cl_8]I$ was also synthesized successfully with the use of Ga_2I_6 or SnI_4 in place of GeI_2.

Structure Determination. Single-crystal X-ray diffraction data were collected at 100 K on an APEX2 diffractometer equipped with graphite-monochromatized Mo Kα (λ = 0.710 73 Å) radiation.[18] The crystal-to-detector distance was 60 mm; the exposure time was 10 s/frame. Collection of intensity data and cell refinement were performed using APEX2 as a series of 0.3° scans in φ and ω.[18] Data reduction was performed by the program APEX2.[18] Face-indexed absorption, incident beam, and decay corrections were performed by the program SADABS.[19] The structure was solved and refined with the use of the SHELX-13 suite of programs.[19,20] Atom positions were standardized using the program STRUCTURE TIDY.[21] Crystallographic images were made using the program CRYSTALMAKER.[22] Further details are given in Table 1 and the Supporting Information.

Optical Measurements. Optical transmission measurements were collected using an inverted Nikon Ti2000-U microscope as previously described.[23−25] A face-indexed $Cs_5[U_2(\mu\text{-}S_2)_2Cl_8]I$ single crystal was mounted on a glass fiber, which was manually positioned above the 40× extra-long working distance objective using a goniometer affixed

Received: January 30, 2015
Published: March 2, 2015

DOI: 10.1021/acs.inorgchem.5b00234
Inorg. Chem. 2015, 54, 3055−3060

Table 1. Crystallographic Data for $Cs_5[U_2(\mu\text{-}S_2)_2Cl_8]I$

cryst syst	orthorhombic
space group	D_{2h}^{25}-*Immm*
a/Å	7.3866(1)
b/Å	10.3524(2)
c/Å	17.1864(4)
V/Å^3	1314.23(4)
T/K	100
Z	2
$R(F)$ $[I > 2\sigma(I)]^a$	0.043
$R_w(F_o^2)^b$	0.174

$^aR(F) = \sum||F_o| - |F_c||/\sum|F_o|$ for $F_o^2 > 2\sigma(F_o^2)$. $^bR_w(F_o^2) = \{\sum[w(F_o^2 - F_c^2)^2]/\sum wF_o^4\}^{1/2}$ for all data. $w^{-1} = \sigma^2(F_o^2) + (0.0533F_o^2)^2$ for $F_o^2 \geq 0$; $w^{-1} = \sigma^2(F_o^2)$ for $F_o^2 < 0$.

to a custom mount. The crystal was oriented with the [010] crystal axis collinear with the optical axis of the objective. A 200 μm pinhole placed in the collection path isolated a 5 μm region of interest at the objective focal plane. Transmittance spectra with and without the crystal at the objective focus were collected for 0.07 s, accumulated 200 times, and corrected for background signal through subtraction of a lamp-off spectrum. Absorbance spectra were calculated from the transmittance spectra. Measurements were performed with a linear polarizer below the tungsten halogen lamp. The polarizer was rotated 360 deg in 10-degree increments to probe the polarization dependence of absorption.

Raman measurements were collected using the same geometry. Excitation of 785 nm was focused onto the crystal through the same objective, and a half-wave plate was used to rotate the incident polarization. Room-light contamination was eliminated by subtracting spectra acquired with the laser blocked. Acquisition conditions: P_{ex} = 2.5 mW, t_{acq} = 10 s, spectra accumulated 18 times.

Magnetics. As no single crystals of suitable size for magnetic measurements were grown, 28.8 mg of single crystals of $Cs_5U_2S_4Cl_8I$ obtained from the synthesis that involved SnI_4 were ground. An X-ray powder diffraction (XRPD) pattern of this sample did not reveal the presence of impurities. Magnetic susceptibility on the resultant powder was measured using a Quantum Design MPMS SQUID magnetometer. The sample was loaded into a gelatin capsule. The data were taken under zero-field-cooled (ZFC) or field-cooled (FC) conditions. No difference between ZFC and FC was observed. About three months after these magnetic measurements the sample, which had been stored under ambient conditions, was re-examined by higher resolution XRPD and EDX methods. These indicated the presence not only of $Cs_5U_2S_4Cl_8I$ but also of CsCl, CsI, SnS_2, S, and UO_2. It was not possible to quantify their relative amounts. Whereas the nonmagnetic impurities (CsCl, CsI, SnS_2, and S) are from the synthesis route, the magnetic impurity (UO_2) is likely from the decomposition of the compound.

RESULTS AND DISCUSSION

Synthesis. $Cs_5[U_2(\mu\text{-}S_2)_2Cl_8]I$ was synthesized from the reaction of U, GeI_2, and S in a CsCl flux at 1173 K. Successful syntheses were also achieved by substituting Ga_2I_6 or SnI_4 for GeI_2. The reactions yielded red plates of $Cs_5[U_2(\mu\text{-}S_2)_2Cl_8]I$ in about 75 wt % yield as well as excess flux and binary byproducts. Attempts to synthesize the Se or Te analogues by substituting Se or Te for S were unsuccessful; U/Q binaries resulted.

Crystal Structure of $Cs_5[U_2(\mu\text{-}S_2)_2Cl_8]I$. The compound $Cs_5[U_2(\mu\text{-}S_2)_2Cl_8]I$ crystallizes in the space group D_{2h}^{25}-*Immm* of the orthorhombic system in the $Cs_5[Nb_2(\mu\text{-}S_2)_2Cl_8]Cl$[26] structure type with two formula units in a cell of dimensions a = 7.3866(1) Å, b = 10.3524(2) Å, and c = 17.1864(4) Å. The structure is composed of two crystallographically independent Cs sites (site symmetries (Cs1 (*m*..), Cs2 (*mmm*)), one U (*mm*2), one S (..*m*), two Cl (Cl1 (.*m*.), Cl2 (*m*..)), and one I (*mmm*)). The formula charge balances with Cs^+, U^{4+}, S_2^{2-}, Cl^-, and I^-.

$Cs_5[U_2(\mu\text{-}S_2)_2Cl_8]I$ is isostructural with the Nb^{4+} compounds $Cs_5[Nb_2(\mu\text{-}S_2)_2X_8]X$ (X = Cl, Br).[26] The Nb compounds were not prepared by high-temperature solid-state methods, but rather $(NMe_4)_4[Nb_2S_4(NCS)_8]$ was dissolved in hot concentrated HX followed by the addition of a solution of CsX in concentrated HX.

The structure of $Cs_5[U_2(\mu\text{-}S_2)_2Cl_8]I$ (Figure 1) is composed of $[U_2(\mu\text{-}S_2)_2Cl_8]^{4-}$ anions, Cs^+ cations, and isolated I^- anions. The centrosymmetric $[U_2(\mu\text{-}S_2)_2Cl_8]^{4-}$ anion (Figure 2) in the structure has crystallographically imposed *mmm* symmetry with the two U^{4+} atoms separated by 3.747(1) Å. Each U atom is coordinated to four Cl atoms and four S atoms from two S_2^{2-} groups in a square-antiprismatic arrangement. Table 2 lists interatomic distances. The U−Cl distances of 2.659(2) and

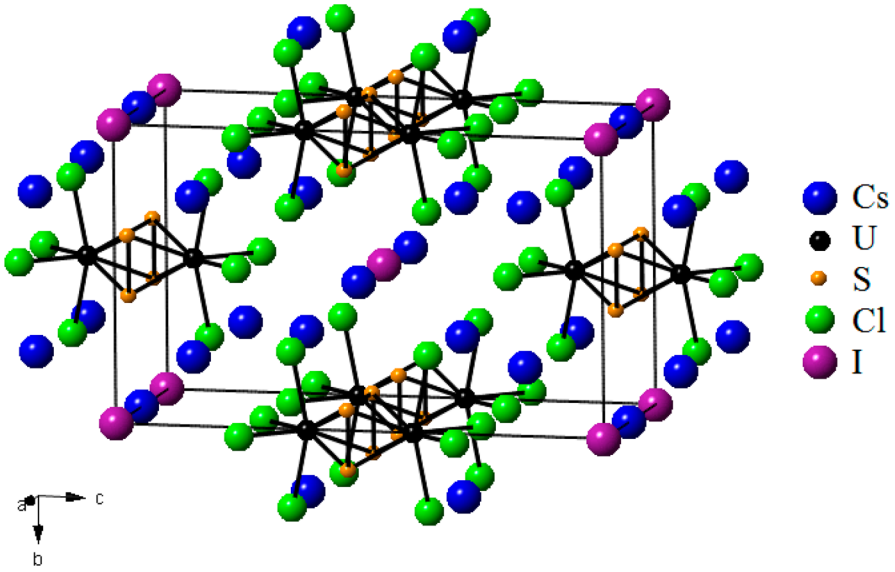

Figure 1. Structure of $Cs_5[U_2(\mu\text{-}S_2)_2Cl_8]I$ viewed approximately along *a*.

DOI: 10.1021/acs.inorgchem.5b00234
Inorg. Chem. 2015, 54, 3055−3060

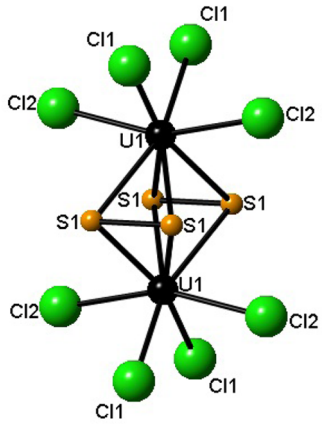

Figure 2. $[U_2(\mu\text{-}S_2)_2Cl_8]^{4-}$ anion of symmetry *mmm*.

Table 2. Selected Interatomic Distances in $Cs_5[U_2(\mu\text{-}S_2)_2Cl_8]I$

	distance (Å)
U1−Cl1 × 2	2.659(2)
U1−Cl1 × 2	2.737(3)
U1−S1 × 4	2.806(2)
U1···U1	3.747(1)
U1···Cs1 × 2	4.639(1)
U1···Cs1	4.700(1)
S1−S1	2.072(6)
U···U[a]	7.387(1)

[a]Shortest U−U interanion distance.

2.737(3) Å and the U−S distance of 2.806(2) Å compare favorably with the corresponding distances in $UTa_2O(S_2)_3Cl_6$,[11] which has U−Cl distances of 2.759(3) to 2.805(3) Å and U−S distances from 2.819(3) to 2.928(3) Å. The S−S distance of 2.072(6) Å in the present compound may be compared with those of 2.077(4) to 2.081(4) Å in $UTa_2O(S_2)_3Cl_6$. The Cs−Cl distances are also comparable: 3.446(3) to 3.711(1) Å; 3.408(3) to 3.673(1) Å in $UTa_2O(S_2)_3Cl_6$.

The $[U_2(\mu\text{-}S_2)_2Cl_8]^{4-}$ anion closely resembles the complex anions in the $[M_2(\mu\text{-}S_2)_2X_8]^{2-}$ (M = Mo, W; X = Cl, Br) salts.[27,28] These compounds contain M^{5+}. This increased charge leads to shorter M−M distances when compared with the Nb analogues. The Nb−Nb distance of 2.924(3) Å in $Cs_5[Nb_2(\mu\text{-}S_2)_2X_8]X$ is, of course, shorter than the U−U distance of 3.747(1) Å in $Cs_5[U_2(\mu\text{-}S_2)_2Cl_8]I$. The related actinide compound $ThTe_2I_2$[17] was synthesized by a combination of the elements at 773 K. In its structure there is a $[Th_2(\mu\text{-}Te_2)_2I_8]^{4-}$ anion cluster that is analogous to the $[U_2(\mu\text{-}S_2)_2Cl_8]^{4-}$ anion in $Cs_5[U_2(\mu\text{-}S_2)_2Cl_8]I$. The Th−Th distance in $ThTe_2I_2$ is 4.057(1) Å.

That the structure of $Cs_5[U_2(\mu\text{-}S_2)_2Cl_8]I$ contains discrete $[U_2(\mu\text{-}S_2)_2Cl_8]^{4-}$ anions is unusual. In general, actinide chalcogenides display structures with infinite chains, layers, or three-dimensional frameworks.[1,4] Notable exceptions to this generalization include four uranyl chalcogenides,[29−31] K_4USe_8,[32] and $K_5U(PS_4)_3$,[33] all of which have isolated U polyhedra. Uranium oxides also show a preference for structures with infinite chains, sheets, or three-dimensional frameworks,[34] but recently a number of compounds with discrete anions have been synthesized with the use of peroxides as bridging ligands.[35] In particular, the structure of $Na_2Rb_4(UO_2)_2(O_2)_5(H_2O)_{14}$[36] contains uranyl peroxide molecular dimers with O_2^{2-} bridging ligands that are analogous to the S_2^{2-} units seen in $Cs_5[U_2(\mu\text{-}S_2)_2Cl_8]I$.

Optical Properties. The polarized absorbance spectra of $Cs_5[U_2(\mu\text{-}S_2)_2Cl_8]I$ display prominent optical anisotropy (Figure 3). Spectra collected with illumination polarized

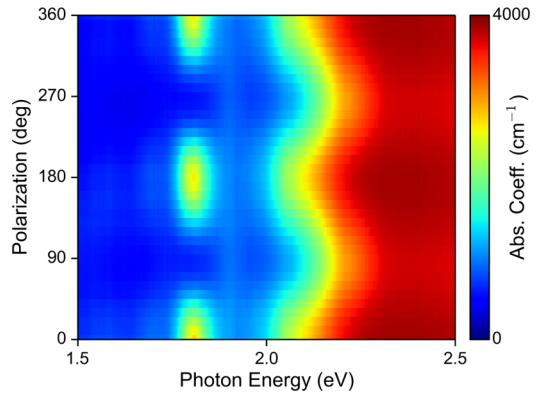

Figure 3. Absorption coefficient of $Cs_5[U_2(\mu\text{-}S_2)_2Cl_8]I$ plotted as a function of energy and incident polarization. 0° corresponds to polarization along the [001] crystal axis, and 90° corresponds to polarization along the [100] crystal axis.

along the [001] crystal axis exhibit a prominent, narrow feature at 1.81 eV, toward the red of the sharp band edge observed. Upon a 90-degree rotation of the incident polarization to the direction of the [100] crystal axis, this sharp feature disappears, and the band edge shifts toward the blue.

The absorbance functions $(\alpha h\nu)^{1/2}$ and $(\alpha h\nu)^2$ were analyzed to characterize the nature of the transitions along both polarization directions (Figure 4).[37] The greater linearity of the band edge in the $(\alpha h\nu)^2$ plots as compared with the $(\alpha h\nu)^{1/2}$ plots suggests direct optical transitions for both polarizations.[37,38] Extrapolation of linear fits of the baselines and band edges in the $(\alpha h\nu)^2$ plots leads to band gaps of 1.99 and 2.08 eV along the [001] and [100] polarizations, respectively.

Polarization anisotropy was also observed in Raman spectra of $Cs_5[U_2(\mu\text{-}S_2)_2Cl_8]I$ (Figure 5). Specifically, bands at 205, 234, 277, and 522 cm^{-1} were prominent with incident polarization parallel to the [100] crystal axis but were suppressed with polarization parallel to the [001] axis. No [001] polarization-specific Raman bands were apparent. Future theoretical work may help elucidate physical explanations for the observed polarization anisotropy.

Magnetic Properties. Figure 6 shows the temperature dependence between 2 and 300 K of the magnetic susceptibility χ (= m/H) of $Cs_5[U_2(\mu\text{-}S_2)_2Cl_8]I$ at different fields. On the whole, χ increases with cooling except in a small region around 60 K, where a local broad peak is observed. The position of this peak decreases with the magnetic field, as shown in the inset of Figure 6. Although UOS has long-range antiferromagnetic ordering at T_N = 55 K[39−41] near this 60 K anomaly, no UOS was detected by XRPD or EDX measurements. Nevertheless undetected amounts of magnetic impurities are always of concern in magnetic measurements. UO_2 was detected in the X-ray powder diffraction pattern taken months after the magnetic measurements. UO_2 is antiferromagnetic (T_N = 30 K),[42] but no anomaly is seen near 30 K.

DOI: 10.1021/acs.inorgchem.5b00234
Inorg. Chem. 2015, 54, 3055−3060

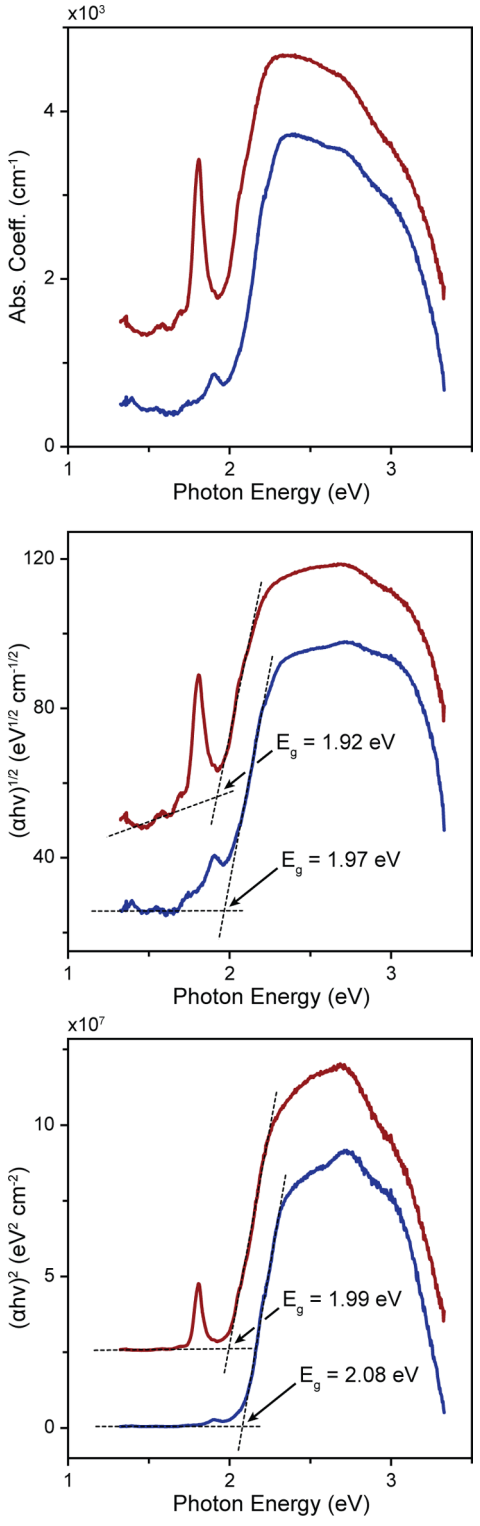

Figure 4. For a single crystal of $Cs_5[U_2(\mu\text{-}S_2)_2Cl_8]I$ the absorption coefficient (A), calculated spectra for an indirect transition (B), and calculated spectra for a direct transition (C) plotted as a function of energy. Spectra collected with light polarized along the [001] and [100] crystal axes are plotted in red and blue, respectively.

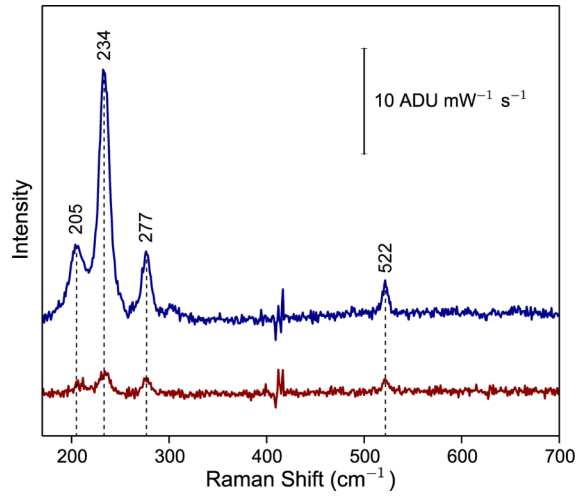

Figure 5. Normal Raman spectra of $Cs_5[U_2(\mu\text{-}S_2)_2Cl_8]I$. Spectra collected with light polarized along the [001] and [100] crystal axes are plotted in red and blue, respectively.

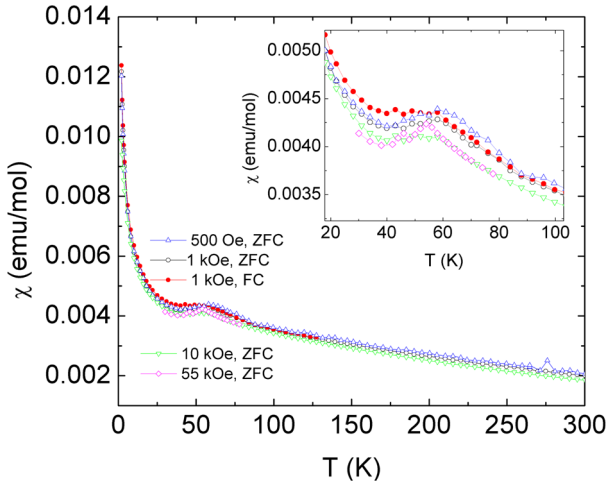

Figure 6. Temperature dependence of the magnetic susceptibility χ of $Cs_5[U_2(\mu\text{-}S_2)_2Cl_8]I$ at different fields between 2 and 300 K. The inset shows in more detail the region between 20 and 100 K.

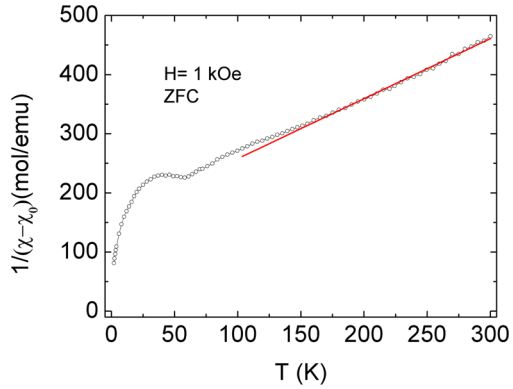

Figure 7. $1/(\chi - \chi_0)$ vs T for the 1 kOe ZFC data of $Cs_5[U_2(\mu\text{-}S_2)_2Cl_8]I$.

Above 150 K the temperature dependence of χ can be fit with the modified Curie–Weiss law, $\chi = C/(T - \theta_W) + \chi_0$, where C is the Curie constant, θ_W is the Weiss temperature, and χ_0 is the temperature-independent susceptibility. Figure 7 presents a plot of the inverse susceptibility $1/(\chi - \chi_0)$ vs T for the 1 kOe ZFC data. Figure 8 shows the magnetization data at 2 and 5 K. These show no sign of hysteresis or saturation at the measured field range. From the susceptibility data we obtained $\mu_{eff} = 1.97(2)\ \mu_B$, $\theta_W = -150(3)$ K, and $\chi_0 = -1.5 \times 10^{-4}$ emu/

DOI: 10.1021/acs.inorgchem.5b00234
Inorg. Chem. 2015, 54, 3055–3060

mol, where μ_{eff}, the effective magnetic moment, is given by $\mu_{eff} = (7.997C)^{1/2}$. The negative Weiss temperature implies an antiferromagnetic interaction between magnetic ions. χ_0 is diamagnetic and of similar order to the combined contribution of core diamagnetism using Pauli's constant (-5.4×10^{-4} emu/mol) and the magnetic moment of the empty sample holder (-1.7×10^{-5} emu at 1 kOe). Thus, there is a small paramagnetic background in addition to the known diamagnetic sources. As noted above, X-ray powder diffraction results on the sample performed about three months after the magnetic measurements indicate the presence of CsCl, CsI, SnI_2, S, and UO_2. The unknown masses of these possible impurities render the value of μ_{eff} of 1.97(2) μ_B a lower limit. The free U^{4+} ion with Russell–Saunders coupling has a magnetic moment of 3.6 μ_B. The value of χ_0 would be uncertain if UO_2 were present in the measured sample.

The nearest distance between the U^{4+} ions of 3.747(1) Å is within the $[U_2(\mu\text{-}S_2)_2Cl_8]^{4-}$ anion. All other U···U distances are 7.387 Å or greater. The intra-anion U–U distance is close to the Hill limit[43] (~3.5 Å), below which overlap of 5f electrons creates itinerant electrons and prevents magnetic ordering. The observed magnetic susceptibility is consistent with the modified Curie–Weiss law at high temperatures, which implies that at high temperatures the magnetism is dominated by separated U^{4+} ions. On the other hand, it is possible that the U^{4+} ions within the $[U_2(\mu\text{-}S_2)_2Cl_8]^{4-}$ anion may be responsible for the observed magnetic susceptibility at low temperatures. Thus, dimerized spins could result from antiferromagnetic coupling between the U^{4+} ions within the cluster below 60 K. The dimerization not being perfect would leave a finite moment at each cluster site. Then, the Curie–Weiss law would govern the magnetic susceptibility at low temperatures, as the finite moment of the anions can be treated as independent because of the long interanion distance. When the modified Curie–Weiss law was applied to the 1 kOe ZFC data below 10 K, we obtained $\mu_{eff} = 0.5\ \mu_B$, which corresponds to 0.71 ($=0.5 \times \sqrt{2}$) μ_B per anion after the partial dimerization.

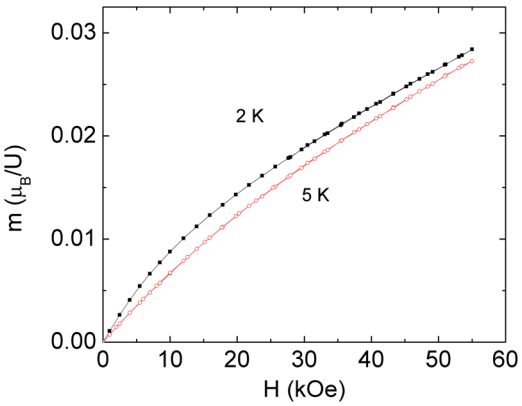

Figure 8. Magnetization (m) as a function of field (H) for $Cs_5[U_2(\mu\text{-}S_2)_2Cl_8]I$.

CONCLUSIONS

$Cs_5[U_2(\mu\text{-}S_2)_2Cl_8]I$ was synthesized in good yield from the reaction of U, GeI_2, and S in a CsCl flux at 1173 K. Successful syntheses were also achieved by substituting Ga_2I_6 or SnI_4 for GeI_2. Attempts to synthesize the Se or Te analogues by substituting Se or Te for S were unsuccessful; U/Q binaries resulted.

The compound $Cs_5[U_2(\mu\text{-}S_2)_2Cl_8]I$ crystallizes in space group D_{2h}^{25}-*Immm* of the orthorhombic system in the $Cs_5[Nb_2(\mu\text{-}S_2)_2Cl_8]Cl$[26] structure type. The structure of $Cs_5[U_2(\mu\text{-}S_2)_2Cl_8]I$ is composed of $[U_2(\mu\text{-}S_2)_2Cl_8]^{4-}$ anions, Cs^+ cations, and isolated I^- anions. The centrosymmetric $[U_2(\mu\text{-}S_2)_2Cl_8]^{4-}$ anion in the structure has *mmm* symmetry with the two U^{4+} atoms separated by 3.747(1) Å. Each U atom is coordinated to four Cl atoms and four S atoms from two S_2^{2-} groups in a square-antiprismatic arrangement. The formula charge balances with Cs^+, U^{4+}, S_2^{2-}, Cl^-, and I^-.

The polarized absorbance spectra of $Cs_5[U_2(\mu\text{-}S_2)_2Cl_8]I$ display prominent optical anisotropy. The direct optical transitions for polarizations along the [001] and [100] crystal directions lead to band gaps of 1.99 and 2.08 eV, respectively.

The observed magnetic susceptibility is consistent with the modified Curie–Weiss law at high temperatures, which implies that at high temperatures the magnetism is dominated by separated U^{4+} ions. On the other hand, it is possible that the U^{4+} ions within the $[U_2(\mu\text{-}S_2)_2Cl_8]^{4-}$ anion may be responsible for the observed magnetic susceptibility at low temperatures.

ASSOCIATED CONTENT

Supporting Information

Crystallographic file in CIF format for $Cs_5[U_2(\mu\text{-}S_2)_2Cl_8]I$. This material is available free of charge via the Internet at http://pubs.acs.org.

AUTHOR INFORMATION

Corresponding Author

*E-mail: ibers@chem.northwestern.edu.

Notes

The authors declare no competing financial interest.

ACKNOWLEDGMENTS

Use was made of the IMSERC X-ray facility at Northwestern University, supported by the International Institute of Nanotechnology. Funding for optical measurements was provided by the National Science Foundation Grant CHE-1152547 and the NSF MRSEC Grant DMR-1121262. This material is based upon work supported by the National Science Foundation Graduate Research Fellowship under Grant No. DGE-1324585. A portion of this work was performed at the National High Magnetic Field Laboratory, which is supported by NSF Cooperative Agreement No. DMR-1157490 by the State of Florida and by the DOE. Any opinions, findings, and conclusions or recommendations expressed in this material are those of the authors and do not necessarily reflect the views of the National Science Foundation.

REFERENCES

(1) Manos, E.; Kanatzidis, M. G.; Ibers, J. A. In *The Chemistry of the Actinide and Transactinide Elements*, 4th ed.; Morss, L. R.; Edelstein, N. M.; Fuger, J., Eds.; Springer: Dordrecht, The Netherlands, 2010; Vol. 6, pp 4005–4078.
(2) Bugaris, D. E.; Ibers, J. A. *Dalton Trans.* **2010**, *39*, 5949–5964.
(3) Koscielski, L. A.; Ibers, J. A. *Z. Anorg. Allg. Chem.* **2012**, *638*, 2585–2593.
(4) Narducci, A. A.; Ibers, J. A. *Chem. Mater.* **1998**, *10*, 2811–2823.
(5) Noel, H.; Troc, R. *J. Solid State Chem.* **1979**, *27*, 123–135.

DOI: 10.1021/acs.inorgchem.5b00234
Inorg. Chem. 2015, 54, 3055–3060

(6) Malliakas, C. D.; Yao, J.; Wells, D. M.; Jin, G. B.; Skanthakumar, S.; Choi, E. S.; Balasubramanian, M.; Soderholm, L.; Ellis, D. E.; Kanatzidis, M. G.; Ibers, J. A. *Inorg. Chem.* **2012**, *51*, 6153−6163.
(7) Cody, J. A.; Ibers, J. A. *Inorg. Chem.* **1995**, *34*, 3165−3172.
(8) Bugaris, D. E.; Choi, E. S.; Copping, R.; Glans, P.-A.; Minasian, S. G.; Tyliszczak, T.; Kozimor, S. A.; Shuh, D. K.; Ibers, J. A. *Inorg. Chem.* **2011**, *50*, 6656−6666.
(9) Neuhausen, C.; Rocker, F.; Tremel, W. *Z. Anorg. Allg. Chem.* **2012**, *638*, 405−410.
(10) Mesbah, A.; Stojko, W.; Malliakas, C. D.; Lebegue, S.; Clavier, N.; Ibers, J. A. *Inorg. Chem.* **2013**, *52*, 12057−12063.
(11) Wells, D. M.; Chan, G. H.; Ellis, D. E.; Ibers, J. A. *J. Solid State Chem.* **2010**, *183*, 285−290.
(12) Ward, M. D.; Klingsporn, J. M.; Ibers, J. A. *Inorg. Chem.* **2013**, *52*, 10220−10222.
(13) Bugaris, D. E.; Ibers, J. A. *J. Solid State Chem.* **2008**, *181*, 3189−3193.
(14) Wells, D. M.; Ibers, J. A. *Z. Anorg. Allg. Chem.* **2010**, *636*, 440−442.
(15) Beck, J.; Fischer, A. *Z. Anorg. Allg. Chem.* **2002**, *628*, 369−372.
(16) Sawodny, V.; Rediess, K.; Thewalk, U. *Z. Anorg. Allg. Chem.* **1983**, *499*, 81−88.
(17) Rocker, F.; Tremel, W. *Z. Anorg. Allg. Chem.* **2001**, *627*, 1305−1308.
(18) Bruker *APEX2* Version 2009.5-1 Data Collection and Processing Software; Bruker Analytical X-Ray Instruments, Inc.: Madison, WI, USA, 2009.
(19) Sheldrick, G. M. *SADABS*; Department of Structural Chemistry, University of Göttingen: Göttingen, Germany, 2008.
(20) Sheldrick, G. M. *Acta Crystallogr. Sect. A: Found. Crystallogr.* **2008**, *64*, 112−122.
(21) Gelato, L. M.; Parthé, E. *J. Appl. Crystallogr.* **1987**, *20*, 139−143.
(22) Palmer, D. *CrystalMaker Software* Version 2.7.7; CrystalMaker Software Ltd.: Oxford, England, 2013.
(23) Koscielski, L. A.; Pozzi, E. A.; Van Duyne, R. P.; Ibers, J. A. *J. Solid State Chem.* **2013**, *205*, 1−4.
(24) Mesbah, A.; Lebegue, S.; Klingsporn, J. M.; Stojko, W.; Van Duyne, R. P.; Ibers, J. A. *J. Solid State Chem.* **2013**, *200*, 349−353.
(25) Ward, M. D.; Pozzi, E. A.; Van Duyne, R. P.; Ibers, J. A. *J. Solid State Chem.* **2014**, *212*, 191−196.
(26) Sokolov, M.; Imoto, H.; Saito, T.; Fedorov, V. *Z. Anorg. Allg. Chem.* **1999**, *625*, 989−993.
(27) Fenske, D.; Czeska, B.; Schumacher, C.; Schmidt, R. E.; Dehnicke, K. *Z. Anorg. Allg. Chem.* **1985**, *520*, 7−17.
(28) Virovetz, A. V.; Slovokhotov, Y. L.; Struchkov, Y. T.; Fedorov, V. E.; Mironov, Y. V.; Fedin, V. P. *Koord. Khim.* **1990**, *16* (2), 198−202.
(29) Sutorik, A. C.; Kanatzidis, M. G. *Polyhedron* **1997**, *16*, 3921−3927.
(30) Grant, D. J.; Weng, Z.; Jouffret, L. J.; Burns, P. C.; Gagliardi, L. *Inorg. Chem.* **2012**, *51*, 7801.
(31) Perry, D. L.; Zalkin, A.; Ruben, H.; Templeton, D. H. *Inorg. Chem.* **1982**, *21*, 237.
(32) Sutorik, A. C.; Kanatzidis, M. G. *J. Am. Chem. Soc.* **1991**, *113*, 7754−7755.
(33) Hess, R. F.; Abney, K. D.; Burris, J. L.; Hochheimer, H. D.; Dorhout, P. K. *Inorg. Chem.* **2001**, *40*, 2851−2859.
(34) Burns, P. C. *Can. Mineral.* **2005**, *43*, 1839−1894.
(35) Qiu, J.; Burns, P. C. *Chem. Rev.* **2013**, *113*, 1097−1120.
(36) Kubatko, K.-A.; Forbes, T. Z.; Klingensmith, A. L.; Burns, P. C. *Inorg. Chem.* **2007**, *46*, 3657−3662.
(37) Bang, T.-H.; Choe, S.-H.; Park, B.-N.; Jin, M.-S.; Kim, W.-T. *Semicond. Sci. Technol.* **1996**, *11*, 1159−1162.
(38) Deng, B.; Chan, G. H.; Huang, F. Q.; Gray, D. L.; Ellis, D. E.; Van Duyne, R. P.; Ibers, J. A. *J. Solid State Chem.* **2007**, *180*, 759−764.
(39) Ballestracci, R.; Bertaut, E. F.; Pauthenet, R. *J. Phys. Chem. Solids* **1963**, *24*, 487−491.
(40) Amoretti, G.; Blaise, A.; Caciuffo, R.; Fournier, J. M.; Larroque, J.; Osborn, R. *J. Phys.: Condens. Matter* **1989**, *1*, 5711−5720.
(41) Troc, R.; Zolnierek, Z. *J. Phys. (Paris)* **1979**, *C4*, 79−81.
(42) Frazer, B. C.; Shirane, G.; Cox, D. E.; Olsen, C. E. *Phys. Rev.* **1965**, *140*, A1448−A1452.
(43) Hill, H. H. In *Plutonium 1970 and Other Actinides*; Miner, W. N., Ed.; The Metallurgical Society of the American Institute of Mining, Metallurgical, and Petroleum Engineers, Inc.: New York, NY, 1970; Vol. *17*, pp 2−19.

DOI: 10.1021/acs.inorgchem.5b00234
Inorg. Chem. 2015, 54, 3055−3060